Alternative work roll material grade for the late-finishing stands of hot strip mills

Davison Nyabadza[1,2], and *Charles Witness* Siyasiya[2]

[1] South African Roll Company, South Africa.
[2] Department of Material Science and Metallurgy Engineering, University of Pretoria South Africa.

Abstract. The ever-increasing demand for high productivity and strip surface quality in hot strip mills (HSMs) has been the driving force in the search for work rolls with excellent wear and mill incidence resistance. Indefinite chill double pour rolls (ICDPs), which are currently applied to the late finishing stands (LFS) due to their superior mill incidence resistance, exhibit relatively poor wear resistance. The inferior wear resistance negatively impacts mill productivity due to frequent mill stoppages. The superb wear resistance of high-speed steel (HSS) rolls is attributed to the presence of discrete high hardness carbides. A potential work roll for the LFSs presenting improved wear and mill incidence resistance was designed using Thermo-Calc software. The alloy was melted in an induction furnace and centrifugally cast into sleeves. Specimens from the sleeves were tempered at various temperatures. Characterisation of both as-cast and heat-treated samples involved chemical, microstructural (OM), SEM-EBSD, XRD), hardness and Ferritscope measurements. The amount and distribution of graphite particles was comparable to ICDPs. The microstructure consisted of graphite nodules, carbides and retained austenite (RA) in a tempered martensitic matrix. Hardness values up to 63HRC with <3% residual austenite (RA) were obtained, which makes this grade more superior to ICDPs.

1 Introduction

Rolling involves the reduction of a workpiece or material's thickness by passing it between a pair of work rolls rotating or turning in opposite directions. The reduction in thickness with each pass results in a proportional increase in length to conserve volume. Rolling is categorized as cold or hot depending on the temperature of the workpiece and it accounts for at least 90% of all metal-forming processes. [**1-4**]. Hot rolling, which is of interest to this paper, results in a net increase in strength, toughness and ductility. An equiaxed grain structure is also obtained with hot rolling. Slabs, blooms and billets can be rolled into various finished and semi-finished products such as plates, strips, structural sections, bars and rails as shown in Figure 1.

The processing of a slab into a strip or sheet is a hot rolling operation carried out in hot strip mills (HSMs). A conventional configuration of an HSM is shown in Figure 2 which consists of a reheating furnace (RF), roughing mill (RM), finishing mill (FM) and a down coiler (DC).

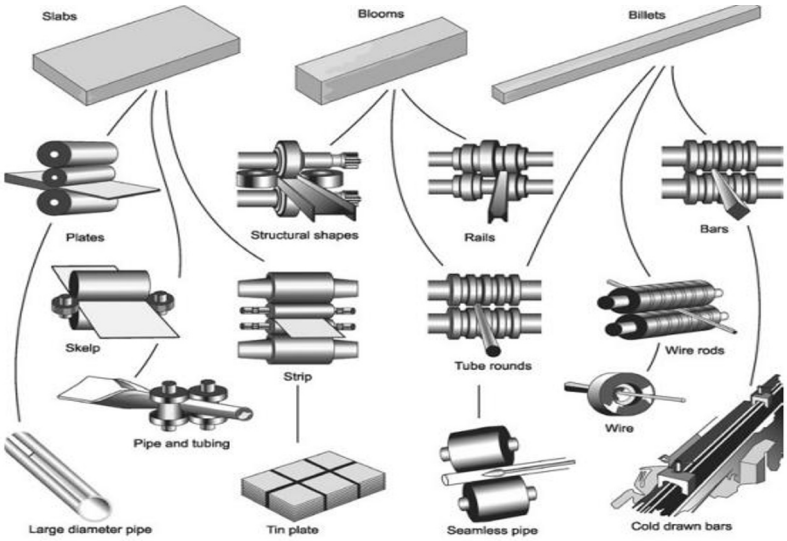

Fig. 1. Schematic presentation of flat and shape metal rolling processes [4].

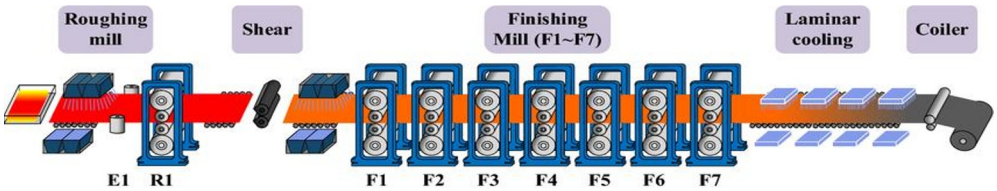

Fig. 2. Schematic layout of a hot strip mill [5].

HSMs can be classified as integrated, mini or Steckel mills [**6**]. Integrated HSMs can have continuous, semi-continuous or reverse roughing trains and up to 7 finishing train stands [**6-8**]. The FM is divided into early (F1~F4) and late finishing stands (F5~F7). Work rolls suitable for the early finishing stands should possess high resistance to thermal fatigue with high fracture toughness and wear since they are in contact with the plate for the longest time while late finishing stand rolls should withstand abrasive wear and mechanical fatigue [**8,9**]. Three main roll grades used are high chromium iron (HCI), high speed steel (HSS) and indefinite chill (IC) also known as indefinite chill double pour (ICDP) [**9-11**], Figure 3.

The ever-increasing demand for higher productivity and product quality has been the driving force in the search for new and improved roll material grades. ICDPs have been historically used in all finishing stands but were replaced in the EFS with HCI rolls in the late 1960s. The introduction of HSS rolls in the early 1990s saw the progressive replacement of HCI and ICDP rolls in the early finishing stands [**6,10,12-15**]. Wear resistance of HSS rolls is 4 and 5 times higher than that of HCI and ICDP respectively [**13,16,17**] resulting in a 250% increase in campaign lengths [**16**]. Oda et al [**13**] reported that HSS rolls achieve 5000-10000 tons compared to about 1500-2000 tons for ICDPs before grinding.

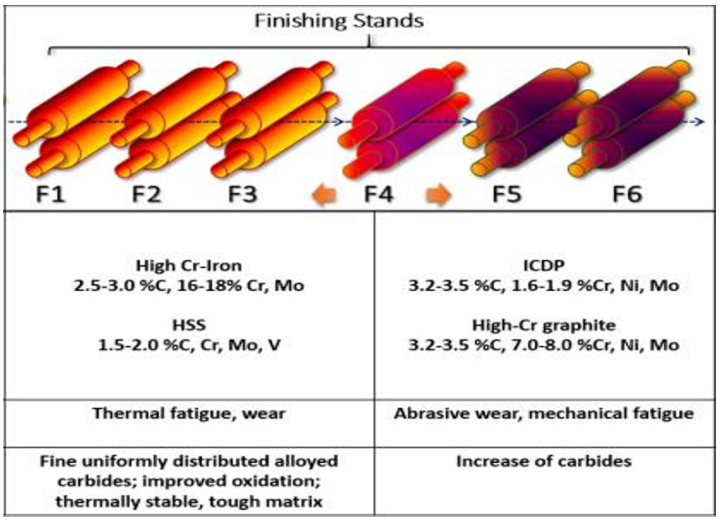

Fig. 3: Typical work rolls for the finishing stands of a HSM [9].

The superior wear resistance of HSS rolls is attributed to the presence of sufficient amounts of very hard and discrete MC, M_6C and M_2C eutectic carbides [**2**,**11,18,19**]. The LFS stands are characterised by rolling mill incidents such as cobbles, crimps, sticking and folded and whipping tail ends due to higher rolling speeds and thinner gauges [**2**,**13,18,20,21**] leading to partial or total loss of work roll life [**21**]. Early trials (in Europe and Japan) with HSS rolls in rear finishing stands were abruptly halted due to the high sensitivity of these rolls to mill incidents [**20**]. Despite the higher wear resistance, HSS rolls have not been able to replace ICDP rolls in the LFSs due to poor anti-sticking and anti-cracking properties [**13**].

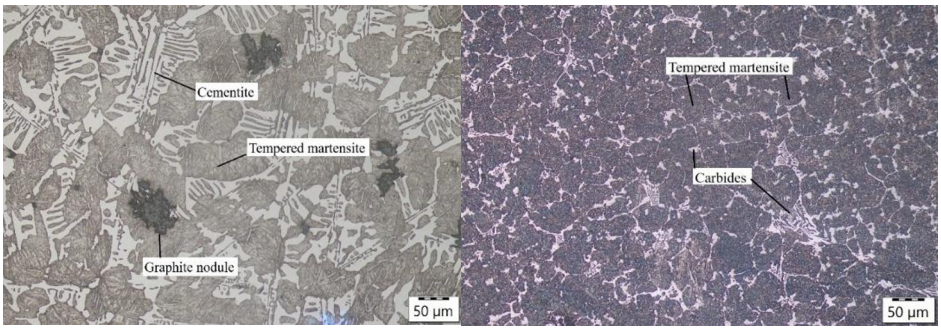

(a) (b)

Fig. 4. a) ICDP micrograph showing carbides (cementite) and graphite in a tempered martensitic matrix and **(b)** micrograph of HSS showing carbides in a tempered martensitic matrix.

The inferior wear resistance of ICDP rolls in the LFSs increase the frequency of mill stoppages due to roll grinding and changing thus hampering mill productivity [**13,16,22**]. Doubling the performance of ICDP work rolls in the late finishing stands would allow for synchronised roll changes thereby improving the mill's productivity [**13**]. Enhancement of conventional ICDPs with carbide formers such as vanadium (V) and niobium (Nb) increased the wear performance by 10-50% [**13,20,22**] which was considered a minor step in terms of performance improvement. Mill incidence resistance of ICDP rolls is attributed to the presence of crystallised or free graphite which acts as a lubricant thereby preventing sticking

while improving thermal behaviour and retarding crack propagation [**10,13,14,23**]. Figure 4 shows typical microstructures of HSS and ICDP rolls used in the EFS and LFS of FMs respectively.

Trials on graphitised HCI were abruptly stopped due to performance well below expectation. This shifted the focus in the last decade to graphitised grades which could achieve wear resistance comparable to HSS roll grades. Superior wear and mill incidents resistance has been reported in industrial trials of graphitised HSS roll grades [**13,22,24**]. Literature on potential materials to replace ICDPs in the late-finishing stands is still very limited. The South African Roll Company (SARCO) seeks to develop a graphitised material grade for the late-finishing stands to replace carbide enhanced ICDP roll grades. Hence, this study focused on the development of a material which combines properties exhibited by both HSS and ICDP rolls.

2 Materials and methods

2.1 Thermo-Calc simulation

Thermo-Calc software was used to simulate solidification behaviour of various material compositions. One alloy composition which showed potential to precipitate a balanced amount of graphite and carbides was selected for further processing. Table 1 shows the chemical composition of the alloy in weight %. The main alloying elements included carbon (C), manganese (Mn), silicon (Si), nickel (Ni), chromium (Cr), molybdenum (Mo), vanadium (V) and niobium (Nb).

Table 1. Chemical composition in wt.% of the selected alloy.

C	Mn	Si	Ni	Cr	Mo	V + Nb
1.5-4.0	0.5-2.0	0.8-5.2	3.0-6.0	1.0-3.5	0.5-5.0	0.5-5.0

2.2 Melting and horizontal spincasting

Charge material with a total weight of 1500 kgs was melted in a 3-Ton coreless induction furnace. Each charge consisted of steel scrap, pig iron and ferro-alloys. Furnace samples were taken after melt out followed by correction of the chemical composition. The molten metal was tapped and poured into a chill rotating at 400-600 rpm (Figure 5a). The spincast process was completed in 25 minutes. The sleeve was allowed to cool down to around 150°C before extraction (Figure 5b). The sleeve was broken into pieces which could be handled by a sample cut-off machine. The specimens were approximately 15 mm thick and 15 to 20 mm long.

(a) (b)

Fig. 5. (**a**) Solidified sleeve inside the chill and **(b**) sleeve extracted from the chill.

2.3 Material characterisation

Both unetched and etched micrographs were viewed and captured using an Olympus BX41M optical microscope (OM) with a Nikon Digital Sight Image Analyser. The Olympus Stream Imaging Analysis software was utilised in phase quantification. The amount of graphite was evaluated in the unetched condition while the total carbides was measured after etching the specimen with 3% Nital solution. The scanning electron microscope, SEM (JOEL JSM-IT300LV) equipped with energy dispersive spectroscopy (EDS), was used for the identification of various phases.

The hardness was measured using an Emcotest DuraJet hardness testing machine with a digital display. The hardness measurements of the as-cast material were taken up to a depth of 40 mm. The indentations of the heat-treated material were done closer to the center or middle of the specimens. All hardness values were reported in Rockwell C (HRC).

A Fischer Ferritscope FMP30 with a FGAB 1.3-Fe probe was used to determine the degree of ferricity on flat surfaces of specimens. The instrument measures non-destructively the total amount of the alpha (α) and delta (δ) ferrite using the magnetic induction technique. Increases in %Fe values are observed when samples are tempered indicating the relative degrees of transformation of austenite to bainite or martensite.

2.4 Heat treatment

Specimens were batched and heat treated in a Heraeus Laboratory Furnace with a maximum operating temperature of 1150°C. Three tempering temperatures (namely T, T+50 and T+100) ranging between 400 and 600°C were selected. Tempering was completed for each tempering temperature when the RA was <5%. A heating rate of 10°C/min was applied on all cycles for durations ranging from 2 to 10 hours.

3 Results and discussions

3.1 Thermo-Calc simulation results

The software predicted precipitation of graphite, carbides, austenite and ferrite (Table 2). MC-type carbides of V and Nb constituted 8.6% volume fraction. The total quantity of molybdenum carbides (Mo_2C) was 5.6% with 5% graphite. The simulation revealed that

niobium carbides (NbC) precipitate first in the liquid phase. Figure 6 shows the alloy's liquidus and solidus temperatures of 1210 and 1140°C respectively.

Table 2. Quantitative analysis of phases predicted.

Phase	Vol. fraction, %
MC (FCC_A1#2 &3)	8.6
M_2C/M_6C (M_6C)	5.6
Graphite	5.1
Austenite (FCC_A1)	5.3
Ferrite (BCC_A2)	75.3

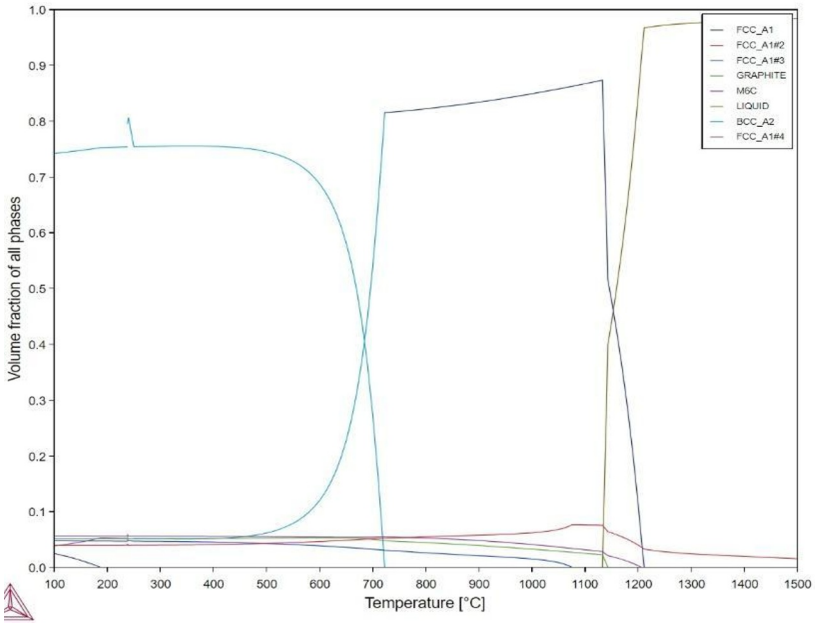

Fig. 6. Thermo-Calc simulation predicting volume fractions of various phases under equilibrium conditions.

3.2 As-cast microstructures and hardness values

Optical micrographs for the as-cast developed alloy are shown in Figure 7. The unetched micrographs show precipitated graphite nodules. An average amount of 1.2% graphite was measured using the image analysis. The amount, shape and distribution of graphite was comparable to that of enhanced ICDP grades manufactured by SARCO which vary from 0.8 to 3% depending on the type of mill and the required hardness. The volume fraction of carbides across the depth of 40 mm was observed to be between 16 and 22% i.e., less than that of enhanced ICDP rolls which is typically between 25 to 35%. The carbides' structure was found to be relatively finer and discrete compared to ICDP grades (Figure 4b). Figure 8

is a SEM micrograph showing graphite nodules and carbides in an untempered martensitic matrix.

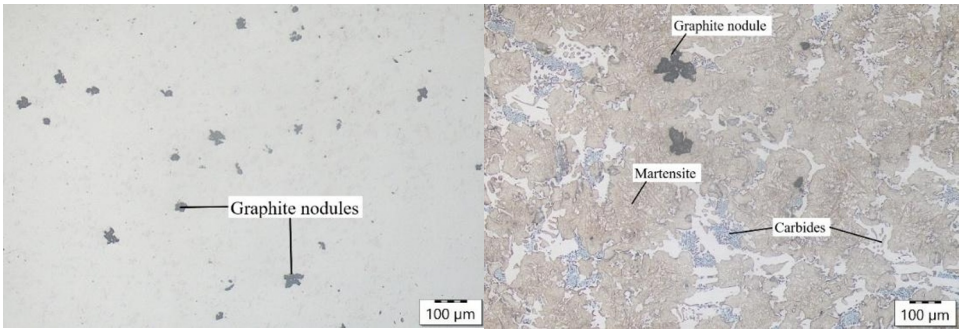

(a) (b)

Fig. 7. (**a**) Unetched OM photo showing graphite nodules (black) and **(b)** etched OM photo showing graphite nodules (black) and carbides (white) in a martensitic matrix.

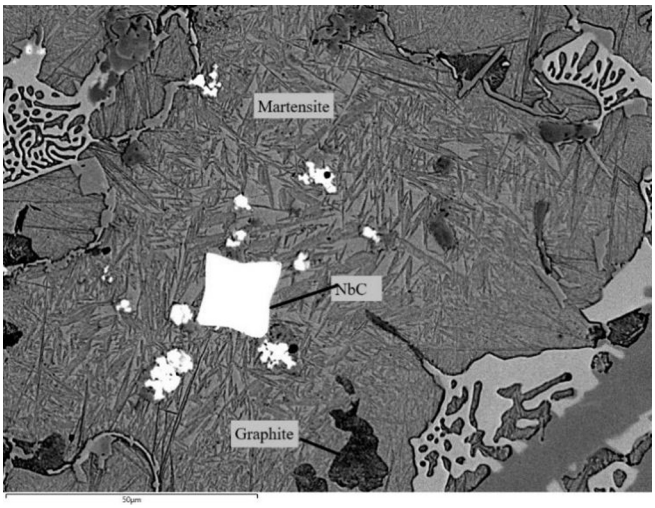

Fig. 8. As-cast SEM image showing graphite and carbides in an untempered martensitic matrix.

The variation in hardness and % Ferrite with depth of the shell was found to be trivial, Figure 9. The average hardness achieved of 61.5 HRC was above the minimum required hardness of 58 HRC. Typical hardness values for conventional and enhanced-carbide ICDP grades range between 55 and 60 HRC. Ferritscope measurements as "% Ferrite" slightly increased with shell depth from the outer surface at 40% to 42.5% at 35mm which represent the volume fraction of RA from 13 to 11.7 respectively. The volume fraction of the RA was found to be approximately 12% along the depth of the shell. The typical Ferritscope values for as-cast ICDP grades range between 45 and 50. The relatively lower %Ferrite reveal that the amount of RA in the new grade is more than that of ICDPs. This suggests that higher

tempering temperatures or longer tempering times could be required to decrease the amount of RA to acceptable levels of less than 5%.

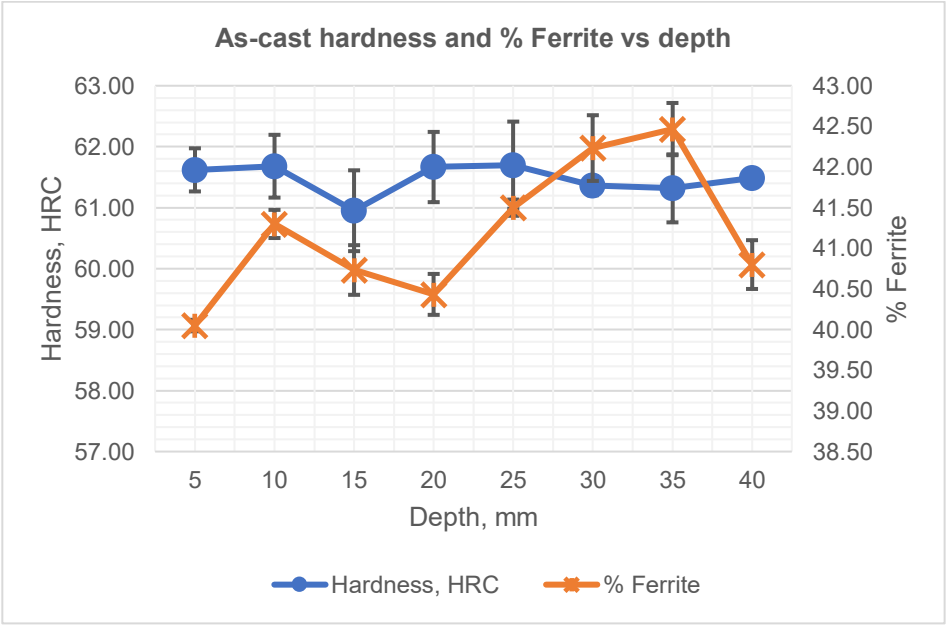

Fig. 9. Hardness and % Ferrite from 5 to 40mm depth of as-cast specimen.

3.3 Heat-treated microstructures and hardness values

The OM and SEM micrographs after the tempering heat treatment are shown in Figure 10. The microstructures are comparable to the as-cast (shown in Figure 7). Noticeable differences include very fine secondary carbides and a tempered martensitic matrix.

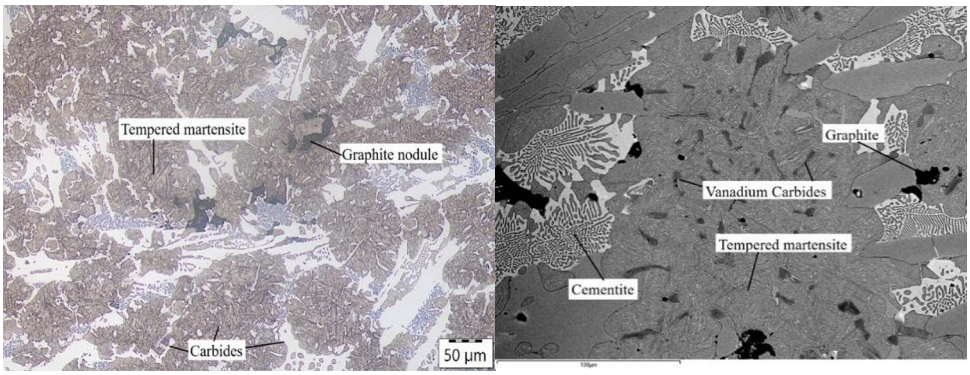

(a) (b)

Fig. 10. (**a**) OM and **(b)** SEM micrographs after tempering showing various phases.

However, the increase in the volume fraction of the carbides was insignificant. Vanadium enriched carbides were observed (VC) as also found in HSS rolls, Figure 10 b. Comparison of Figure 10 b to Figure 8 reveal the effect of tempering on martensite and RA.

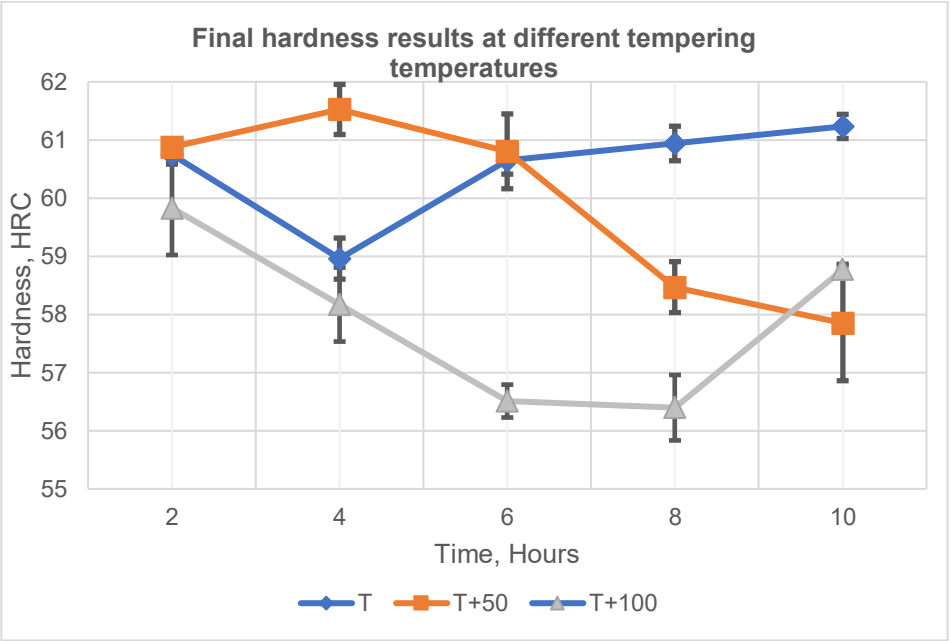

Fig. 11. Change in hardness on the last tempering cycle for each temperature.

A general increase in hardness with each tempering cycle was observed leading to an increase of 1 HRC (see Figure 11). The increase in hardness was attributed to the secondary precipitation of very fine carbides. The Ferritscope value of 59.3 was measured after the third temper cycle which indicates that the amount of RA was less than 3%, Figure 12. The implication is that the material's proneness to spalling during rolling is significantly reduced.

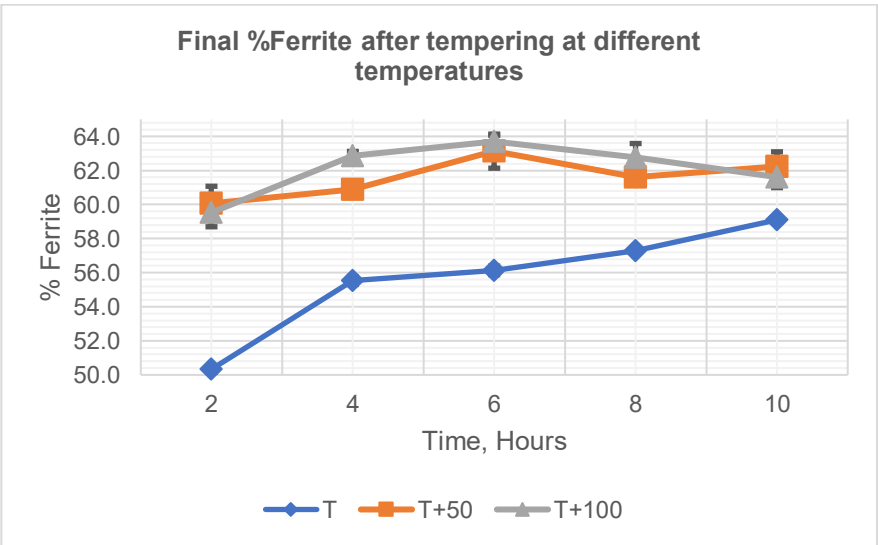

Fig. 12. Hardness and % ferrite values after the third temper cycle.

4 Conclusions

The development of an alternative work roll to ICDP rolls in the late-finishing stands of hot strip mills achieved desired and promising results. The developed alloy contained approximately 1.2% nodular graphite which improves mill incidence resistance and anti-sticking properties which are critical for work rolls in the rear finishing stands. The presence of appreciable amounts of discrete high hardness carbides (MC and M_2C-type) and higher overall hardness significantly improves wear resistance and performance during rolling. Spalling resistance of the new grade is expected to be comparable to that of CDP grades since the amount of RA (3%) after tempering is in the same range. Triple tempering at 450°C for 10 hours was found to be optimal to achieve acceptable RA content.

The authors would like to acknowledge technical and financial assistance from the South African Roll Company (SARCO) and the Department of Material Science and Metallurgical Engineering at the University of Pretoria for providing research facilities.

References

1. O.M. Ikumapayi, E.T. Akinlabi, P. Onu, O.P. and Abolusoro, Rolling operation in metal forming: process and principles- a brief study, Mat. Today: Proc. **26**, 1644-1649 (2020)

2. W.L. Roberts, Mechanical principles of rolling process. Iron & St. Soc. Publ. 215-265 (2002)

3. S. Ramasamy, Analysis of rolling. MSc Thesis Ohio University (1988)

4. S. Ray, Principles and applications of metal rolling, Cambridge Univ. Press, 1-10

5. Z. Wang, Y. Liu, T. Wang, D. Gong & D. Zhang, Prediction model of hot strip crown based on industrial data and hybrid the PCA-SDWPSO-ELM approach, **27**, 12483–12499 (2023)

6. R. Webber, Preferred roll specification for rolling ferrous materials in hot strip mills. Iron & St. Soc. Publ. 289-307 (2002)

7. M. Brandner, T. Nylen, and A. Paar, Indefinite chill cast iron rolls and future possibilities. Technical contribution to the 50th rolling seminar- processes, rolled and coated products. 18-21 November 2013, Ouro Preto, Brazil. 1-10 (2013)

8. F.J. Belzunce, A. Ziadi, and C. Rodriguez, Structural integrity of hot strip mill rolling rolls. Eng. Failure Anal. **11**. 789-797 (2004)

9. K.V. Redkin, Development and microstructural improvement of spin cast high-speed steel rolls. PhD Dissertation, University of Pittsburgh, USA (2013)

10. L. Hao, Z.Y. Jiang, D.B. Wei, H. Wu, X.W. Cheng, J.W. Zhao, S.Z. Luo, and L.Z. Jiang, Wear and friction behaviour of high-speed steel and indefinite chill material for rolling ferritic stainless steel, Research online, University of Wollongong, 1- 13 (2017)

11. M. Nilsson, and M. Olsson, An investigation of worn work roll materials used in the finishing stands of the hot strip mill for steel rolling. Proc. of the Inst. of Mech. Eng. Part j, Jour. Eng. Trib., 1-11 (2013)

12. M. Boccalini Jr, and A. Sinatora, Microstructure and wear resistance of high speed steels for rolling mill rolls. 6th Int. Tool. Conf., 509-52 (2002)

13. N. Oda, P. Fleiner, and H. Tushiyuki, Latest developments of a new technology hss work roll for later stands (f4-f7) in hot strip mill finishing trains, AIST, Pittsburgh, 56-62 (2013)

14. J. Lecomte-Beckers, L. Terziev, and J.P. Breyer, Graphitisation in chromium cast iron. the iron and steel society: 39th Mech. Work. Steel Proc. Conf., Indianna, USA, 1-10 (1997)

15. R.W. Kaiser, S. Mehlau, J. Kruger, L. Hellenthal and I. Oberding, IRLE'S HSS grade for F5-7 work rolls. 51st Roll. Sem. Proc., rolled and coated prod. Foz do Iguacu, Brazil, 168-177 (2014)

16. H. Takigawa, S. Ohtomo, T. Tanaka and M. Hashimoto, Development of high-speed tool steel rolls and their application to rolling mills. Nippon steel Tech. **74**, 77-83 (1997)

17. H. Fu, A. Zhao and J. Xing, Development of centrifugal casting high speed steel rolls. Jour. Univ. of Sc. Tech. Beijing, **10** (No.6), 61-66 (2003)

18. K. Yamamoto, T. Harakawa and K. Ogi. The role of alloying elements in high speed steel type cast irons. Int. Jour. Cast Met. Res. **11**, 297-301 (1999)

19. J. Lecomte-Beckers, J.T. Tchuindjang, E. Pirard and J-P. Breyer, Physical metallurgy of hss material for hot rolling mill rolls. Univ. of Liege, Belgium. 1-10 (2002)

20. S. Flament, G. Walmag, O. Lemaire and M. Sinnaeve, Characterizations, modelling and lab trials assisting the development of a graphitic hss work roll for the rear finishing stands. SARUC 2017. 26-27 Oct 2017, Vanderbijlpark, South Africa. 19-25 (2017)

21. C.R. Serantoni, N.L. dos Santos, G.D. Paulo, M.M. Matsumoto and G.T. Cornelio, Development of rolling mills rolls with high abrasive wear resistance for the last stands of hot strip mills, SARUC 2017. 26-27 Oct 2017, Vanderbijlpark, South Africa 15-17 (2017)

22. C. Zybill, V. Goryany, J. Buch, O. Myronova and M. Romschied, New graphitized hss materials for rolls in finishing stands. Verlag Stahleisen GmbH, Dusseldorf, 61 -64 (2015)

23. S.V. Bravo, K. Yamamoto, H. Miyahara and K. Ogi, Control of carbide and graphite in cast iron type alloy's microstructures for hot strip mills. Jour. of Met., **2012**, 1-6 (2012)

24. M. Brandner, M. Paar, and S. Mul, New alloying concept for finishing mill rolls including results in application and surface tests. Tech. Metal. Miner. Sao Paulo, 137-148 (2020)